RSC Advances

PAPER

View Article Online
View Journal | View Issue

Cite this: *RSC Adv.*, 2019, **9**, 40031

Synthesis of pyrrolo[3′,2′:4,5][1,3]diazepino[2,1,7-*cd*]pyrrolizine derivatives from dicyanovinylene-bis(*meso*-aryl)dipyrrin†

Ji-Young Shin *

Received 28th October 2019
Accepted 22nd November 2019

DOI: 10.1039/c9ra08850d

rsc.li/rsc-advances

Pyrrolo[3′,2′:4,5][1,3]diazepino[2,1,7-*cd*]pyrrolizine derivatives **2** and **3** were synthesized from dicyanovinylene-bis(*meso*-aryl)dipyrrin in the presence of either $BF_3 \cdot OEt_2$ or $InBr_3$, where **2** was readily oxidized in aerobic conditions to be **3**. It was understood that the fully elongated π-conjugation of **3** is achieved *via* the conformation of **2**. Crystal structures of **2** and **3** were elucidated by X-ray diffraction analysis. Furthermore, two redox states, $\mathbf{3}_{ox}$ and $\mathbf{3}_{red}$ were observed in the chemical redox processes.

Introduction

Dipyrrins are useful molecular units to produce neutral metal-chelating complexes and also enables pigments to build up enlarged π-electron conjugations.[1] Bisdipyrrins, two-dipyrrin-linked molecules, have been employed as appropriate building blocks to form assembling molecules by non-covalent bonding interfaces like metal-chelating and hydrogen bonding interactions, whose subsequent assemblies often stimulated the formation of structures, such as helixes, zigzag ribbons, 2D sheets, and tunnels.[2] There is ongoing research about how solvent molecules or gas-phase molecules act as guest molecules within the assembled structures. Furthermore, some of the structures have been promoted to devise materials for ion/proton channels due to their efficient electrochemical behaviors.[3] Bisdipyrrins have been also induced in enlarged π-conjugation molecules like expanded porphyrinoids exhibiting useful unique macrocyclic skeletons, whose molecular functions are capable of a myriad of practical applications such as in chemosensing[4] and for medicinal sciences.[5]

Unique DDQ-adducts are formed in the oxidation of dipyrromethanes containing electron-withdrawing *meso*-aryls, with DDQ (2,3-dichloro-5,6-dicyano-1,4-benzoquinone)[6] and further treatment of the DDQ adducts with Lewis base results in compound **1** (molecular structure in Fig. 1), which was previously reported.[7] It has been reported that the Ni^{II}-metallation of dicyanovinylene-bis(*meso*-aryl)dipyrrin **1** under refluxing toluene conditions results in the formation of a bicyclic pyrrolizine ring which affords two isomeric bisNi^{II} expanded porphyrinoid complexes (reaction shown in Fig. 1).[8] It was deliberated that the Ni^{II} acetate functions as a Lewis acid and a metalizing source in the reaction process. Furthermore, bisNi^{II} complexes have exhibited routine diatropic ring currents of aromatic expanded porphyrinoids. Since then the creation of the macrocycle was associated with the formation of the pyrrolizine platform followed by metal chelation, the uses of nontransition metallic Lewis acids were considered for forming free-base expanded porphyrinoids. A semi-metallic Lewis acid, $BF_3 \cdot OEt_2$ that has often been used as a convenient Lewis-acid, was chosen first. The structure of the resulting product was elucidated by X-ray diffraction analysis, where the formation of a sizeable macrocyclic structure was not found. In contrast, a ring-closing to create pyrrolodiazepinopyrrolizine group arose by the nucleophilic displacement of pyrrole-βH by its neighbouring imine.

Furthermore, a precursor of the final product compound **2** was obtained when a basic metal Lewis acid, $InBr_3$ replaced the

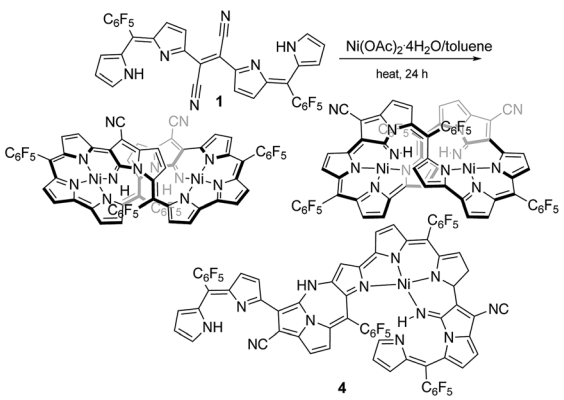

Fig. 1 Formation of stereoisomers of expanded porphyrinoid bisNi^{II} complexes from **1** and a minor product **4**.

Department of Molecular and Macromolecular Chemistry, Graduate School of Engineering, Nagoya University, Furo-cho, Chikusa-ku, Nagoya 464-8603, Japan. E-mail: jyshin@chembio.nagoya-u.ac.jp; Fax: +81-52-747-6771

† Electronic supplementary information (ESI) available: NMR, mass, and absorption spectra as well as X-ray packing diagrams. CCDC 1936172 and 1952976. For ESI and crystallographic data in CIF or other electronic format see DOI: 10.1039/c9ra08850d

Lewis acid ($BF_3 \cdot OEt_2$), which contains a dipyrromethane segment instead of dipyrrin. The molecular structure was also elucidated by X-ray diffraction analysis. The details are reported herein.

Results and discussion

The previous reaction rationalized the formation of expanded porphyrinoid bisNi^{II} complexes (Fig. 1), where a by-product was isolated in an ignorable amount.[5] Nonetheless, the assignment of the molecular structure was successful by crystallographic analysis, which coincided with the structure of compound **4**. From the structure, it was deduced that the generation of pyrrolodiazepinopyrrolizine groups results in incomplete macrocycles. The advanced condensation and metallation were not conducted in the presence of pyrrolo-diazepinopyrrolizine group whose formation drove the two terminal pyrroles apart. Competition between the formations of pyrrolodiazepinopyrrolizine and the large macrocycles happens simultaneously in the synthesis, which probably was the primary reason for the formation of the products. Alternating metal chelation was the other essential factor, which prevented the formation of the unlikely fused rings. In the reaction of **1** with $BF_3 \cdot OEt_2$, compound **3** (Scheme 1) was obtained as almost the quantitative product of the reaction. Both compounds **3** and **4** resulted from the formation of the fused rings (Fig. 2 and S12†).

$BF_3 \cdot OEt_2$ was added to a solution of **1** in a mixed medium of toluene and THF to manage the solubility of both the Lewis acid and **1**. The solution was then refluxed for 1 h under N_2 and then cooled down. Blue metallic solids appeared during the refluxing and the formation of solids completed in an hour. The solution colour almost disappeared with the appearance of the precipitates. The liquid phase was removed by decantation to separate the metallic solids. The solids were then dissolved in a co-solvent of MeOH and CH_2Cl_2. Column chromatography on silica gel gave a polar, blue colour fraction as the major product of the reaction. The growth of the single crystal was successful in a CH_2Cl_2 solution of **3** with a reversible vapour diffusion of CH_2Cl_2 and MeOH. The structure of **3** was elucidated by X-ray diffraction analysis, which exhibited one amino-hydrogen providing an intramolecular hydrogen-bond (Fig. 2). Furthermore, compound **2** was isolated in a reasonable amount (*ca.* 30% yield) succeeded in the reaction proceeding with three molar equivalent $InBr_3$ and the growth of single crystals for X-ray diffraction analysis (Fig. 3).

Both crystal structures of **2** and **3** do not have any amino-H on the tetrafused rings. The crystal structure of **2** showed distortion of planarity due to *meso*-sp^{3}C bridge while **3** exhibited

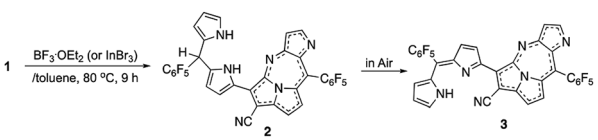

Scheme 1 Formation of **3** from **1** in the presence of selected Lewis acids ($BF_3 \cdot OEt_2$ and $InBr_3$).

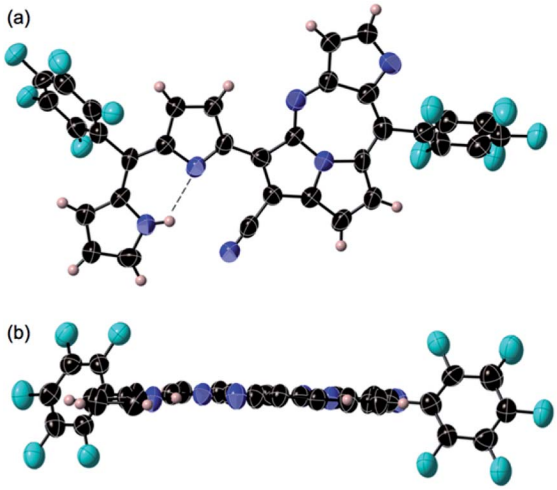

Fig. 2 Crystal structure of **3**: top view (a) and side views (b). Thermal ellipsoids are scaled at the 50% probability level. Two molecules having slightly different planarity and bond alternations were found in the unit and each pair of the enantiomers was observed in the unit cell.

high planarity. In the molecular structure of **3**, an intramolecular hydrogen bond between the amino-group (donor) and the imino-group (acceptor) of the dipyrrin unit was found, which enhanced the planarity of the dipyrrin. Close orientations of the nitrile-N toward the internal hydrogen bond and αC–H of pyrrole toward imino-N of the seven-membered ring were also satisfactory for stabilizing the whole molecular conformation and increasing the planarity. The unit-packing diagram of **3** comprised two types of enantiomeric pairs. The crystallographic analysis of **2** was awarded conclusively in

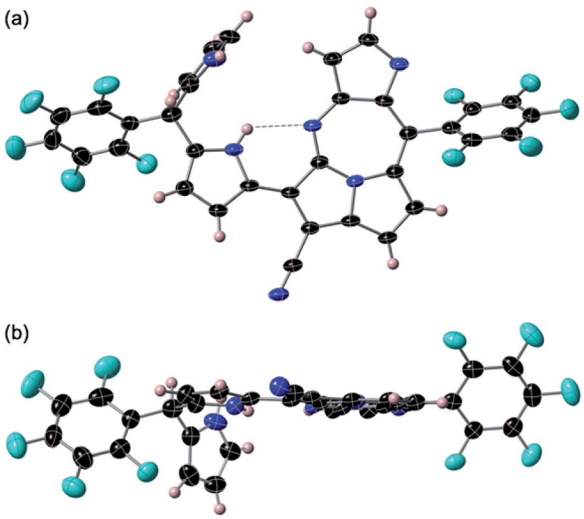

Fig. 3 Crystal structure of **2**: top view (a) and side views (b). Thermal ellipsoids are scaled at the 50% probability level. A pair of enantiomers was observed in the unit cell. The angle between the mean plane of pyrrolo-diazepinopyrrolizine and second pyrrole ring of the dipyrrin and the plane of terminal pyrrole plane placing perpendicularly were measured in 82.60°. NH–N length of the hydrogen bond shown with dashed line is measured in 2.843 Å.

a CH_2Cl_2 solution by vapour diffusion of hexane, in which thin block crystals of **2** were obtained. Nevertheless, **2** was readily oxidized in aerobic conditions to **3**. The terminal pyrrole ring is orthogonal to the mean plane over the pyrrolodiazepinopyrrolizine and internal pyrrole groups due to the repulsion between two hydrogens of amino-groups at the dipyrrin unit, whose angle between the two planes was measured to be 82.60°. The intramolecular hydrogen bond seen at the dipyrrin unit in the structure of **2**, shifted to between an imino-N of the fused linkage created with cyano-origin and the neighbouring pyrrole-NH, which probably is an important factor in the competition for the final molecular stability. The positionally shifted hydrogen bond in the molecular structure of **2** weakened the strength of the hydrogen bonding interaction and the NH–N distance of **2** was measured as 2.843 Å (the distance is relatively longer than that in **3**). An enantiomeric pair was found in the unit cell of **2** since the structure is chiral.

Fig. 4 is the ^{1}H NMR spectra of **1**, **2**, and **3**. As the deliberated formation of a strong intramolecular hydrogen bond between imino-N and the amino-NH in the structure of **3**, a proton peak is shown at a largely downfield area (13.46 ppm) of the spectrum (Fig. 4a). The corresponding proton peak of **2** appeared at a relatively up-field shifted area (11.74 nm), as reflecting a weakened hydrogen bond. Furthermore, the other two amino-NHs of pyrrolodiazepinopyrrolizine group resonated with the proton peaks at 8.41 and 6.12 ppm for pyrrolo-NH and diazepino-NH, respectively (Fig. 4b). Since **2** was readily converted to **3**, a set of the proton peaks of **3** was seen in the ^{1}H NMR spectrum of **2** (the peaks for **3** was distinguished with black dots in the ^{1}H NMR spectrum **4b**). Compared to **3**, αCH of the external pyrrole of **2** resonated the proton peak at a largely up-field shifted area. The αCH peaks were assigned at 8.12 ppm for $\mathbf{3_{ox}}$ and 6.40 ppm for **2**.

Reversible conversions between the two redox-states were observed with absorption spectroscopy engaged with the redox processes (Fig. 5). An irreversible oxidation potential was found at 0.701 V (*vs.* Fc/Fc^+) and one weak and one strong reduction potentials were found in the cyclic voltammogram of $\mathbf{3_{ox}}$. Since two redox states of compound **3** were considered, the reduction potential of −1.403 V was assigned as the reduction conversion from $\mathbf{3_{ox}}$ to $\mathbf{3_{red}}$.

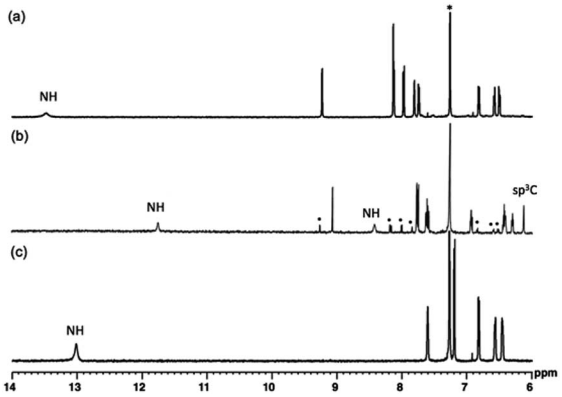

Fig. 4 ^{1}H NMR spectra of **3** (a), **2** (b) and **1** (c) in $CDCl_3$. * are peaks of solvent molecules. Also, the H-peaks distinguished with black dots are for its oxidation state, **3**.

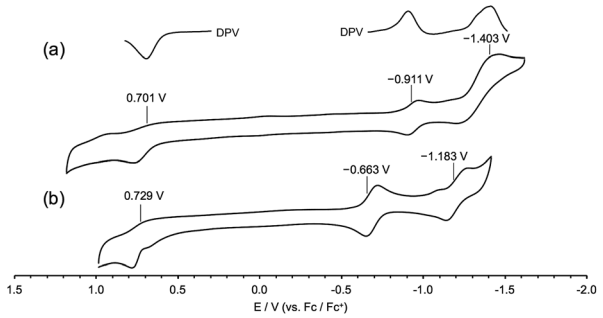

Fig. 5 Cyclic voltammograms of **3** (a) and its precursor **1** (b) in CH_2Cl_2 (0.1 M $^nBu_4NPF_6$). Working electrode: glassy carbon, counter electrode: Pt, reference cell: Ag/AgCl, and Fc/Fc^+: ferrocene/ferrocenium couple.

3 was expected to have two stable redox states, $\mathbf{3_{red}}$ and $\mathbf{3_{ox}}$, as shown in Fig. 6. Since $\mathbf{3_{red}}$ was readily converted to $\mathbf{3_{ox}}$ in solution as well as solid states by oxygen, complete isolation of $\mathbf{3_{red}}$ failed most of the time. While any significant change of the absorption band of $\mathbf{3_{ox}}$ was not observed in chemical oxidation with DDQ (Fig. S17†), the absorption spectrum of $\mathbf{3_{ox}}$ was drastically changed in a chemical reduction with $NaBH_4$ (Fig. 7). In the absorption spectrum of $\mathbf{3_{red}}$, the absorption band of $\mathbf{3_{ox}}$ at around 650 nm was slightly shifted to a longer wavelength and broadened as well as weakened, which appears to contain an absorption shoulder that reaches *ca.* 830 nm. The significant color change of the solution by the reduction was observed from green to purplish-blue, as presented in the corner of Fig. 7.

Theoretical calculation results of the density functions for $\mathbf{3_{ox}}$ and $\mathbf{3_{red}}$ were given in Fig. 8. The HOMO energy level of $\mathbf{3_{ox}}$ (−6.00 eV) is lower than that of $\mathbf{3_{red}}$ (−4.94 eV) and a larger HOMO–LUMO gap is found for $\mathbf{3_{ox}}$ (1.78 eV and 2.18 eV are the values of HOMO–LUMO gaps for $\mathbf{3_{red}}$ and $\mathbf{3_{ox}}$, respectively), thus $\mathbf{3_{red}}$ is converted to $\mathbf{3_{ox}}$ rapidly due to the high stability of $\mathbf{3_{ox}}$. The small HOMO–LUMO gap of $\mathbf{3_{red}}$ supports why its absorption band appears more bathochromic shifted.

Experimental

Materials and methods

All chemicals were purchased from commercial suppliers and used without further purification. Chromatographic

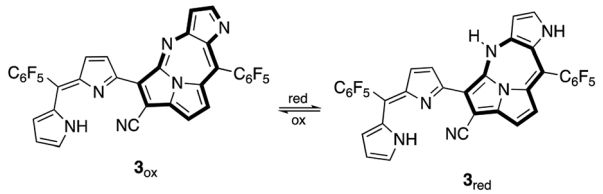

$\mathbf{3_{ox}}$ $\mathbf{3_{red}}$

Fig. 6 Redox conversions of **3**: reduced form ($\mathbf{3_{red}}$) and oxidized form ($\mathbf{3_{ox}}$).

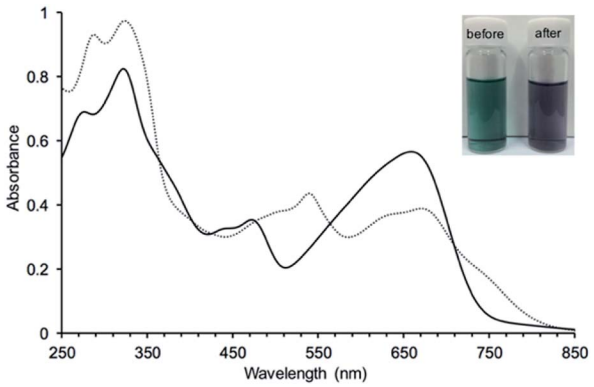

Fig. 7 UV absorption spectral change of **3** in CH_3OH by a reduction with $NaBH_4$: before (—) and after (···) addition of $NaBH_4$. A photograph of the solutions before and after reduction were added in the corner of the spectra as indicating the significant absorption change.

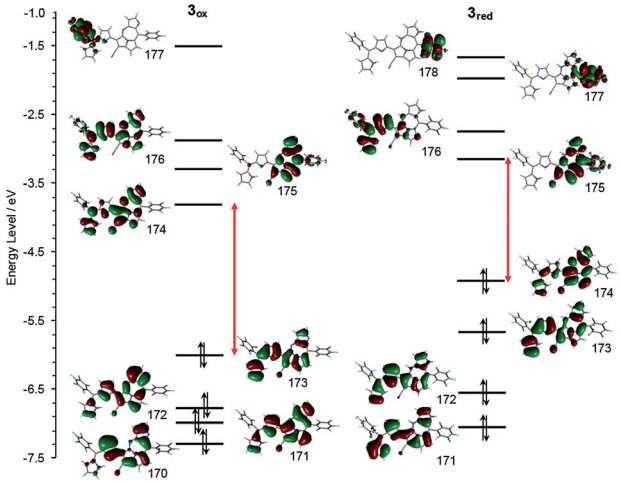

Fig. 8 Frontier MO energy levels of $\mathbf{3}_{ox}$ (left) and $\mathbf{3}_{red}$ (right) calculated at B3LYP/6-311+g(d) level.[9]

separations were carried out by silica gel column chromatography (Silica gel 300) and gel permeation chromatography. NMR data of the compounds were measured with Bruker Avance 300 and 500 MHz NMR spectrometers in $CDCl_3$ solvent, with the use of an internal standard of TMS. The standard Bruker software was used for homonuclear 1D and homonuclear as well as heteronuclear 2D experiments. Cyclic voltammograms were recorded on an ALS electrochemical analyzer 612C. A 0.1 M solution of tetrabutyl-ammonium hexafluorophosphate in CH_2Cl_2 was prepared as the CV electrolyte, and a three-electrode system (a glassy carbon working electrode, a Pt counter electrode, and $Ag/AgClO_4$ reference electrode) was used for the CV measurement. All CV potentials were counted with the reference potential of ferrocene/ferrocenium ion couple. Single crystal diffraction data were collected and integrated, using the Rigaku CCD diffractometer (Saturn 724 with MicroMax-007) with Varimax Mo optics using graphite monochromated Mo-Kσ radiation (Nagoya University). The structure was solved by using direct methods with SHELXS97 and refined by using SHELXL97. All hydrogen atoms were placed in the calculated positions, respectively. All theoretical calculations were provided using the Gaussian 09 program.[9] Optimization of the structures was performed with Becke's three-parameter hybrid exchange functional and Lee–Yang–Parr correlation functional basis sets (B3LYP/6-311+g(d)).

General procedure for the synthesis of compounds 2 and 3

(Method A) $BF_3 \cdot OEt_2$ (100 μL) was added into a toluene (25 mL) solution containing the precursor **1** (50 mg, 0.07 mmol). The reaction mixture was heating overnight in anaerobic condition at 80 °C. While heating, blue precipitates appeared in the solution and the solution became transparent. The resulting solution was then cooled to room temperature and the solvent was removed by decantation. The precipitates were dissolved in $CHCl_3$ and passed through an alumina gel short column with acetone as additional eluent to dissolve the retained precipitates completely. After the initial separation, the second column chromatography was employed using silica gel with $CHCl_3$. The major fraction, green in color, was determined to be **3** (green, 9.8 mg, 20% yield). (Method B) $InBr_3$ (20 mg) was added into a toluene solution of **1** (50 mg, 0.07 mmol) instead of $BF_3 \cdot OEt_2$ with the above reaction condition and the resulting solution was heated overnight at 80 °C. The resulting product solution was washed with water, extracted with CH_2Cl_2, and dried over Na_2SO_4. After removing the solvent by rotary evaporation, the residue was loaded on silica gel and column chromatographed using neat CH_2Cl_2. Green (first) and blue (second) fractions were then separated to obtain **3** and **2**, respectively (27.5 mg (57% yield) and 14.7 mg (30% yield)). The growth of a crystal of **2** was succeeded conclusively in a completely closed system after many times challenges. The identity of the compounds was determined by a ^1H, ^{19}F and ^{13}C-NMR analysis using a $CDCl_3$ solvent and X-ray diffraction analysis of each of crystals. **3** in general organic solvents showed green in colour (dark green powder in the solid-state). **2** in general organic solvents showed blue in colour (dark blue powder in the solid-state).

Spectral data of 2‡

λ_{max} (nm (logε), CH_2Cl_2) 281.5 (4.37), 330.0 (4.44), 475.0 (3.92), 663.5 (4.15); δ_H (300 MHz, 298 K, $CDCl_3$) 11.74 (bs, 1H, NH), 9.06 (d, 1H, $J = 1.8$, βCH), 8.41 (bs, 1H, NH), 7.77 (d, 1H, $J = 1.8$, βCH), 7.75 (d, 1H, $J = 4.5$, βCH), 7.62 (dd, 1H, $^dJ = 4.2$, $^{dd}J = 1.5$, βCH), 7.58 (d, 1H, $J = 4.5$, βCH), 6.93 (dd, 1H, $^dJ = 4.5$, $^{dd}J = 1.8$, βCH), 6.42 (dd, 1H, $^dJ = 5.4$, $^{dd}J = 2.7$, βCH), 6.40 (bs, 1H, αCH), 6.29 (t, 1H, $J = 3.9$, αCH), 6.12 (s, 1H, sp^3CH): the ^1H NMR of **2** showed a small amount of **3** converted by air oxidation even after freshly purified by column chromatography.; δ_F (282.38

‡ Crystallographic data of **2** (CCDC 1936172): $C_{34}H_{12}F_{10}N_6$ $M_r = 694.50$, $T = 93(2)$ K, crystal size = 0.14 × 0.09 × 0.012 mm^3, Mo radiation, monoclinic, space group $P2_1/c$ (#14), $a = 17.8640(10)$ Å, $b = 7.5650(4)$ Å, $c = 20.6477(8)$ Å, $\alpha = 90°$, $\beta = 100.169(5)°$, $\gamma = 90°$, $V = 2746.5(2)$ $Å^3$, $Z = 4$, $P_{calcd.} = 1.680$ g cm^{-1}, $R_1(F) = 0.0799$ ($I > 2(I)$), $wR_2(F^2) = 0.2476$ (all), GoF = 1.029.

MHz, 298 K, $CDCl_3$, calibrated with external CF_3COOH) 137.59 (t, 2F, $^tJ = 19.8$, *o*-CF), 141.33 (d, 2F, $^dJ = 19.8$, *o*-CF),151.21 (t, 1F, $J = 19.8$, *p*-CF), 154.31 (t, 1F, $J = 19.8$, *p*-CF), 160.33 (td, 2F, $^tJ = 22.6$, $^{td}J = 8.47$, *m*-CF), 160.55 (td, 2F, $^tJ = 22.6$, $^{td}J = 8.47$, *m*-CF); *m*/*z* MALDI TOF MS, calcd. for $C_{34}H_{12}F_{10}N_6$ ($[M]^+$): 694.096; found: 694.138.

Spectral data of 3§

λ_{max} (nm (logε), CH_2Cl_2) 275.5 (4.39), 324.0 (4.47), 477.5 (4.12), 668.5 (4.33); δ_H (300 MHz, 298 K, $CDCl_3$) 13.46 (bs, 1H, NH), 9.23 (d, 1H, $J = 1.8$, βCH), 8.13 (d, 1H, $J = 1.7$, βCH), 8.12 (d, 1H, $J = 4.6$, αCH), 7.97 (d, 1H, $J = 4.7$, βCH), 7.81 (bs, 1H, αCH), 7.74 (d, 1H, $J = 4.7$, βCH), 6.83 (d, 1H, $J = 4.7$, βCH), 6.58 (dd, 1H, $^dJ = 4.3$, $^{dd}J = 1.7$, βCH); δ_F (282.38 MHz, 298 K, $CDCl_3$, calibrated with external CF_3COOH) 137.27 (dd, 2F, $^dJ = 19.8$, $^{dd}J = 5.6$, *o*-CF), 137.87 (dd, 2F, $^dJ = 19.8$, $^{dd}J = 5.6$, *o*-CF), 150.85 (t, 1F, $J = 19.8$, *p*-CF), 151.50 (t, 1F, $J = 19.8$, *p*-CF), 160.37 (td, 2F, $^tJ = 19.8$, $^{td}J = 2.8$, *m*-CF), 160.44 (td, 2F, $^tJ = 19.8$, $^{td}J = 2.8$, *m*-CF); δ_C (125.8 MHz, 298 K, $CDCl_3$) 160.56 (sp^2CH), 151.63, 145.95, 143.86, 143.48, 137.59, 137.44, 134.05, 132.94, 131.00, 130.49 (sp^2CH), 126.40 (sp^2CH), 125.01, 124.31 (sp^2CH), 123.72 (sp^2CH), 121.60, 120.08 (sp^2CH), 117.61 (sp^2CH), 117.50 (sp^2CH), 115.38, 111.38, 99.88 (^{13}C peaks of phenyl groups are broaden due to C–F couplings); *m*/*z* MALDI TOF MS, calcd. for $C_{34}H_{10}F_{10}N_6$ ($[M + H]^+$): 693.088, found: 693.127; *m*/*z* APCI HRMS, calcd. for $C_{34}H_{10}F_{10}N_6$ ($[M + H]^+$): 693.0972, found: 693.0880.

Conclusions

Novel pyrrolodiazepinopyrrolizine derivatives **2** and **3** were prepared from a toluene solution of dicyanovinylenebis(*meso*-aryl)dipyrrin **1** at 80 °C, in the presence of specific Lewis acids ($BF_3{\cdot}OEt_2$ and $InBr_3$). Spontaneous oxidation in aerobic conditions readily happens, where complete isolation of the reduced form (**2**) was not successful. However, the reparation of **2** succeeded by the use of $InBr_3$. Elucidation of the structures of both **2** and **3** was accomplished by X-ray diffraction analysis. The structure of **2**, shifted to between an imino-N of the fused linkage created with cyano-origin and the neighboring pyrrole-NH, which probably is an important factor in competitions for the stability of **2**. The crystal structures of **2** and **3** showed two distinct pairs of enantiomers in each of the crystal units. π-electron delocalization happens over the pyrrolodiazepino-pyrrolizine part of **3**, strongly. Two different redox states $\mathbf{3_{ox}}$ and $\mathbf{3_{red}}$ were observed by chemical oxidation with UV/vis absorption spectroscopy. Synthetic investigations towards novel π-conjugation and their characterizations are ongoing in recent research.

§ Crystallographic data of **3** (CCDC 1952976): $(C_{34}H_{10}F_{10}N_6)_2$ $M_r = 1384.96$, $T = 93$ K, crystal size = 0.21 × 0.03 × 0.01 mm^3, Mo radiation, triclinic, space group $P\bar{1}$ (#2), $a = 7.2510(3)$ Å, $b = 18.4847(8)$ Å, $c = 22.9606(10)$ Å, $\alpha = 66.844(4)°$, $\beta = 85.123(3)°$, $\gamma = 87.644(3)°$, $V = 2897.0(2)$ Å^3, $Z = 2$, $P_{calcd.} = 1.588$ g cm^{-1}, $R_1(F) = 0.0747$ ($I > 2(I)$), $wR_2(F^2) = 0.2040$ (all), GoF = 0.949. Squeeze method was used to subtract the electron densities for disordered solvent molecules. The area volume for potential solvent molecules (263.9 Å^3/2897.0 Å^3 (9.1%)) was considered approximately with two methanol molecules.

Conflicts of interest

There are no conflicts to declare.

Acknowledgements

This research was supported by JSPS KAKENHI Grant Number JP18K04925. J.-Y. Shin thanks Prof. Hiroshi Shinokubo for his support of experimental and analytical instruments and his advice. J. Y. Shin also acknowledges the G30 program foundation of Nagoya University for the support of this work.

Notes and references

1 (*a*) C. Brückner, V. Karunaratne, S. J. Rettig and D. Dolphin, *Can. J. Chem.*, 1996, **74**, 2182; (*b*) C. Brückner, Y. Zhang, S. J. Rettig and D. Dolphin, *Inorganica Chim. Acta*, 1997, **263**, 279; (*c*) T. E. Wood and A. Thompson, *Chem. Rev.*, 2007, **107**, 1831; (*d*) L. Yu, K. Muthukumaran, I. V. Sazanovich, C. Kirmaier, E. Hindin, J. R. Diers, P. D. Boyle, D. F. Bocian, D. Holten and J. S. Lindsey, *Inorg. Chem.*, 2003, **42**, 6629; (*e*) G. R. Geier III, J. F. B. Chick, J. B. Callinan, C. G. Reid and W. P. Auguscinski, *J. Org. Chem.*, 2004, **69**, 4159; (*f*) J.-Y. Shin, D. Dolphin and B. O. Patrick, *Cryst. Growth Des.*, 2004, **4**, 661; (*g*) J.-Y. Shin, B. O. Patrick and D. Dolphin, *CrystEngComm*, 2008, **10**, 960; (*h*) C.-H. Lee, F. Li, K. Iwamoto, J. Dadok, A. A. Bothner-By and J. S. Lindsey, *Tetrahedron*, 1995, **51**, 11645; (*i*) *The porphyrin Handbook*, ed. K. M. Kadish, K. M. Smith and R. Guilard, World Scientific Publishing Co. Pte. Ltd., Singapore, 2016, vol. 26; (*j*) R. Taniguchi, S. Shimizu, M. Suzuki, J.-Y. Shin, H. Furuta and A. Osuka, *Tetrahedron Lett.*, 2003, **44**, 2505; (*k*) Q. Li, M. Ishida, H. Kai, T. Gu, C. Li, X. Li, G. Baryshnikov, X. Liang, W. Zhu, H. Ågren, H. Furuta and Y. Xie, *Angew. Chem., Int. Ed.*, 2019, **58**, 5925.

2 (*a*) H. Maeda, H. Hasegawa, T. Hashimoto, T. Kakimoto, S. Nishio and T. Nakanishi, *J. Am. Chem. Soc.*, 2006, **128**, 10024; (*b*) Y. Zhang, A. Thompson, S. J. Rettig and D. Dolphin, *J. Am. Chem. Soc.*, 1998, **120**, 13537; (*c*) A. Thompson, S. J. Rettig and D. Dolphin, *Chem. Commun.*, 1999, 631; (*d*) A. Thompson and D. Dolphin, *Org. Lett.*, 2000, **2**, 1315; (*e*) L. Ma, J.-Y. Shin, B. O. Patrick and D. Dolphin, *CrystEngComm*, 2008, **10**, 1531; (*f*) Q. Miao, J.-Y. Shin, B. O. Patrick and D. Dolphin, *Chem. Commun.*, 2009, 2541; (*g*) Z. Zhang and D. Dolphin, *Chem. Commun.*, 2009, 6931.

3 (*a*) J. R. Pankhurst, N. L. Bell, M. Zegke, L. N. Platts, C. A. Lamfsus, L. Maron, L. S. Natrajan, S. Sproules, P. L. Arnold and J. B. Love, *Chem. Sci.*, 2017, **8**, 108; (*b*) L. Lecarme, A. Kochem, L. Chiang, J. Moutet, F. Berthiol, C. Philouze, N. Leconte, T. Storr and F. Thomas, *Inorg. Chem.*, 2018, **57**, 9708.

4 (*a*) Y. Ding, W.-H. Zhu and Y. Xie, *Chem. Rev.*, 2017, **117**, 2203; (*b*) Q. Zhao, X. Zhou, T. Cao, K. Y. Zhang, L. Yang, S. Liu, H. Liang, H. Yang, F. Li and W. Huang, *Chem. Sci.*, 2015, **6**,

1821; (*c*) Q. H. You, A. W. Lee, W. H. Chan, X. M. Zhu and K. C. F. Leung, *Chem. Commun.*, 2014, **50**, 66207; (*d*) Y. S. Xi, Y. B. Ding, X. Li, C. Wang, J. P. Hill, K. Ariga, W. B. Zhang and W. H. Zhu, *Chem. Commun.*, 2012, 11513; (*e*) B. M. Rambo and J. Sessler, *Chem.–Eur. J.*, 2011, **27**, 4946.

5 (*a*) J. J. Hu, N.-K. Wong, S. Ye, X. Chem, M.-Y. Lu, A. Q. Zha, Y. Guo, A. C.-H. Ma, A. Y.-H. Leung and J. Shen, *J. Am. Chem. Soc.*, 2015, **137**, 6837; (*b*) *B_{12}, vol. 2: Biochemistry and Medicine*, ed. D. Dolphin, John Wiley & Sons, New York, 1982.

6 (*a*) D. Walker and J. D. Hiebert, *Chem. Rev.*, 1967, **67**, 153; (*b*) A. E. Wendlandt and S. S. Stahl, *Angew. Chem., Int. Ed.*, 2015, **54**, 14638; (*c*) L. Capella, P. C. Montevecchi and D. Nanni, *J. Org. Chem.*, 1994, **59**, 7379.

7 J.-Y. Shin, B. O. Patrick and D. Dolphin, *Org. Biomol. Chem.*, 2009, **7**, 2032.

8 N. H. Faialaga, S. Ito, H. Shinokubo, Y. Kim, K. Kim and J.-Y. Shin, *Dalton Trans.*, 2017, **46**, 10802.

9 (*a*) M. J. Frisch, G. W. Trucks, H. B. Schlegel, G. E. Scuseria, M. A. Robb, J. R. Cheeseman, G. Scalmani, V. Barone, B. Mennucci, G. A. Petersson, H. Nakatsuji, M. Caricato, X. Li, H. P. Hratchian, A. F. Izmaylov, J. Bloino, G. Zheng, J. L. Sonnenberg, M. Hada, M. Ehara, K. Toyota, R. Fukuda, J. Hasegawa, M. Ishida, T. Nakajima, Y. Honda, O. Kitao, H. Nakai, T. Vreven, J. A. Montgomery Jr, J. E. Peralta, F. Ogliaro, M. Bearpark, J. J. Heyd, E. Brothers, K. N. Kudin, V. N. Staroverov, R. Kobayashi, J. Normand, K. Raghavachari, A. Rendell, J. C. Burant, S. S. Iyengar, J. Tomasi, M. Cossi, N. Rega, J. M. Milliam, M. Klene, J. E. Knox, J. B. Cross, V. Bakken, C. Adamo, J. Jaramillo, R. Gomperts, R. E. Stratmann, O. Yazyev, A. J. Austin, R. Cammi, C. Pomelli, J. W. Ochterski, R. L. Martin, K. Morokuma, V. G. Zakrzewski, G. A. Voth, P. Salvador, J. J. Dannenberg, S. Dapprich, A. D. Danels, Ö. Farkas, J. B. Foresman, J. V. Ortiz, J. Cioslowski and D. J. Fox, Gaussian. Inc., Wallingford CT, 2009; (*b*) A. D. Becke, *Phys. Rev. A*, 1988, **38**, 3098; (*c*) C. Lee, W. Yang and R. G. Parr, *Phys. Rev. B: Condens. Matter Mater. Phys.*, 1988, **37**, 785.